International Conference on Advanced Mechanics and Renewable Energies ICAMRE2018
November 28 & 29, 2018
Boumerdes - Algeria

Robust Fault Diagnosis of SCARA Industrial Robot Manipulator

Yacine Lounici[1, *], *Youcef* Touati[1], and *Smail* Adjerid[1]

[1]Solid Mechanics and Systems Laboratory (LMSS), Department of Mechanical Engineering, Faculty of Technology (FT), M'hmed Bougara University, Boumerdes 35000, Algeria.

Abstract. Nowadays, robotic systems are being in increasingly demanding in many industrial activities. In order to achieve the maximal performance, complex nonlinear dynamic robotic systems were developed. However, as a consequence, the rate of component malfunctions augments with the complexity of systems. These malfunctions are called faults, which may appear in different parts of the system and can induce changes in the dynamic behaviour. This paper deals with fault diagnosis of a particular kind of industrial robots called selective compliance assembly robot arm (SCARA), where both parameter and measurement uncertainties are taken into account. Residuals and thresholds are generated using the quantitative model-based method. The inverse geometric model is used to find analytical solutions for joints angles and distances given the trajectory of the end effector. The presented geometric model is then used to derive the kinematic model. Using this kinematic model, the robot controller computes the necessary torque applied to each DC servomotor in order to move the robot from the current position to the next desired position. The proposed robust fault diagnosis scheme is then implemented for a SCARA manipulator and simulation results are presented in both normal and faulty situations.

Keywords: SCARA robot, Fault diagnosis, Control, Uncertainties, Modelling.

1 Introduction

The Fault diagnosis of industrial robots is a subject that has been widely investigated in the last years and different methods have been developed. It is well-known that the adoption of successful strategies that are able to diagnose faults in a robot manipulator is widely desired in industrial environments as it might be used to avoid critical situations that may due to the propagation of the faults which affect the actuators, the sensors, or the system parameters of robots. For this reason, this subject motivates many researchers to develop new approaches in order to achieve optimal activities.

In the last years, several approaches have been developed for the so-called qualitative and quantitative methods of fault diagnosis [1, 2]. The qualitative methods are mainly based on artificial intelligence. For example, Jaber et al. [3] proposed the use of discrete wavelet transform in order to decompose signals captured from the manipulator robot into

[*] Corresponding author: yacinelounici7@gmail.com/y.lounici@univ-boumerdes.dz

multiband frequency levels and for each of these levels the standard deviation feature is computed and used to design, and test the neural network for the diagnosis purposes. In [4], the problem of fault diagnosis is solved by forming a stable ARX-Laguerre fuzzy PID system for fault diagnosis of actuator and sensor faults in multi degrees of freedom robot. Another approach based on Neuro-Fuzzy scheme for online FD is developed in [5]. The qualitative model-based FD methods do not require the use of a physical robot model. Nevertheless, most of the aforementioned works are only used for the diagnosis of sensors and actuators faults. The physical parameter faults, such as electrical resistance, or friction coefficient, which can induce changes in the dynamic behaviour of the robotic system, cannot be diagnosed using these approaches. The quantitative approach depends mainly on the accuracy and the quality of the system model, which can be performed by mathematical techniques [6-8]. The latter rely on the analytical redundancy relations (ARRs) generation.

Basically, an ARR is a redundant equation that verifies the coherence between the real system behaviour and a reference behaviour describing the normal operation. These equations can be obtained if the system is observable [9]. Moreover, the ARRs represent the energy conservation equations of the system, and they are systematically obtained by exploitation of the system model. Theoretically, the residuals (r), which are the numerical evaluation of ARRs, are expected to be zero in fault-free case, and different from zero in faulty situations. Nevertheless, due to the imperfect knowledge of the real value of the system parameters and their random variation, a false alarms, non-detections and delays on fault detection may be presented, can cause a degradation of FD performances.

In this paper, a quantitative model-based method is proposed for physical modelling, robust fault diagnosis, residuals and adaptive thresholds generations of particular kind of industrial robots called the selective compliance assembly robot arm (SCARA), where both parameter and measurement uncertainties are taken into account. The SCARA robot is constructed to achieve drilling operations using SolidWorks software, then the obtained model is exported to Matlab/Simulink for position control. Also, the mathematical model of DC servomotors for each joint is included in the control methodology to design PI controllers. The robot malfunctions are detected by comparing residuals to adaptive thresholds. Thus, the proposed method can be used to diagnose the variation of residual signals in each SCARA robot joint arm.

The paper is divided into 5 Sections, after the introduction section, SCARA modelling and control are presented in Section 2. In Section 3 the generation steps of ARRs in the presence of uncertainties using the quantitative model-based method are presented. Section 4 presents the applicability of the proposed method by resorting to a SCARA industrial robot manipulator. Finally, we conclude this work with some suggestions for future works.

2 SCARA robot modelling and control

A horizontal revolute configuration robot, SCARA has four degrees of freedom for drilling task, and it is actuated by four DC servomotors to one vertical (translation of the end effector) and three horizontal (rotation) motions. The difference of study from literature works [10, 11], is differential equations of robot system are not used in the present work and all system dynamics are obtained using the ability of SolidWorks and Matlab/Simulink programs.

In this paper, a four-axis SCARA robot system is designed using SolidWorks software as shown in Fig. 1. The robot is equipped with DC servomotors in each joint, it can generate huge torques but still indicate to system inertia. To remedy this issue, joints are coupled by gears in order to increase torque in the drive shaft. The measurement architecture is composed of a current sensor to measure the current flowing into the DC

motor winding. Information about the current position of the robot joint is obtained by an angular position sensor (Incremental encoder).

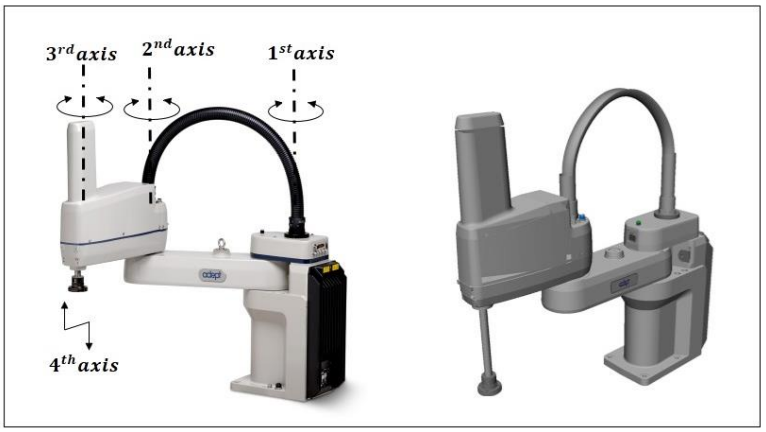

Fig. 1. SCARA industrial robot manipulator design.

2.1 Kinematics and Inverse Kinematics model

In order to obtain the kinematics model, we have considered the Denavit-Hartenberg approach (D-H) [12], whose parameters specified in Fig. 2 are defined in Table 1. We use the standard D-H method to link the coordinate system established at each joint of the transformation matrix that represents its relationship with the previous link coordinate system. Where $\theta_{1,2,3}$ and d_4 are the joint variables.

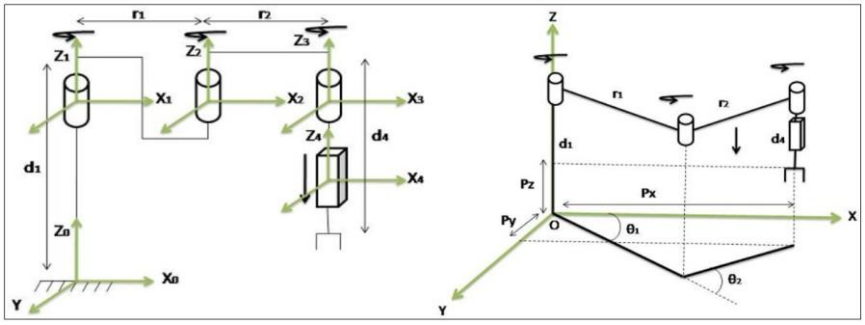

Fig. 2. Denavit-Hartenberg parameters for four joints SCARA robot.

By using (D-H) convention, the transformation matrix representing the position and orientation of frame i relative to $i-1$ is given:

$$ {}^{i-1}M_i = \begin{bmatrix} \cos\theta_i & -\sin\theta_i\cos\alpha_i & \sin\theta_i\sin\alpha_i & r_i\cos\theta_i \\ \sin\theta_i & \cos\theta_i\cos\alpha_i & -\cos\theta_i\sin\alpha_i & r_i\sin\theta_i \\ 0 & \sin\alpha_i & \cos\alpha_i & d_i \\ 0 & 0 & 0 & 1 \end{bmatrix} \quad (1) $$

Then, applying the homogeneous transformations given by Eq. (1), we obtain the matrix (2):

$$ {}^{0}M_4 = {}^{0}M_1.{}^{1}M_2.{}^{2}M_3.{}^{3}M_4 \tag{2} $$

After multiplication and use of addition matrices, one gets the total transformation matrix:

$$ {}^{0}M_4 = \begin{bmatrix} \cos(\theta_1+\theta_2) & -\sin(\theta_1+\theta_2) & 0 & r_1\cos\theta_1 + r_2\cos(\theta_1+\theta_2) \\ \sin(\theta_1+\theta_2) & \cos(\theta_1+\theta_2) & 0 & r_1\sin\theta_1 + r_2\sin(\theta_1+\theta_2) \\ 0 & 0 & 1 & d_1 - d_4 \\ 0 & 0 & 0 & 1 \end{bmatrix} \tag{3} $$

Table 1. Denavit-Hartenberg parameter assignment.

Link i	θ_i	r_i	α_i	d_i
1	θ_1	0	0	d_1
2	θ_2	r_1	0	0
3	θ_3	r_2	0	0
4	0	0	0	$-d_4$

From the elements of the matrix in Eq. (3), position equations (geometric model) are obtained as follows:

$$ p_x = r_1\cos(\theta_1) + \cos(\theta_1+\theta_2) \tag{4} $$

$$ p_y = r_1\sin(\theta_1) + r_2\sin(\theta_1+\theta_2) \tag{5} $$

$$ p_z = d_1 - d_4 \tag{6} $$

From Eqs. (4), (5) and (6), we get:

$$ \dot{p}_x = -r_1\dot{\theta}_1\sin(\theta_1) - r_2(\dot{\theta}_1+\dot{\theta}_2)\sin(\theta_1+\theta_2) \tag{7} $$

$$ \dot{p}_y = r_1\dot{\theta}_1\cos(\theta_1) + r_2(\dot{\theta}_1+\dot{\theta}_2)\cos(\theta_1+\theta_2) \tag{8} $$

$$ \dot{p}_z = -\dot{d}_4 \tag{9} $$

So,

$$ \begin{bmatrix} \dot{p}_x \\ \dot{p}_y \\ \dot{p}_z \end{bmatrix} = \begin{bmatrix} -r_1\sin(\theta_1) - r_2\sin(\theta_1+\theta_2) & -r_2\sin(\theta_1+\theta_2) & 0 \\ r_1\cos(\theta_1) + r_2\cos(\theta_1+\theta_2) & r_2\cos(\theta_1+\theta_2) & 0 \\ 0 & 0 & 1 \end{bmatrix} . \begin{bmatrix} \dot{\theta}_1 \\ \dot{\theta}_2 \\ \dot{d}_4 \end{bmatrix} \tag{10} $$

In order to control the motion of the SCARA robot at the joint rate level, we need the Jacobian matrix, the Jacobian matrix of this case is given by:

$$J(q)=\begin{bmatrix} -r_1\sin(q_1)-r_2\sin(q_1+q_2) & -r_2\sin(q_1+q_2) & 0 \\ r_1\cos(q_1)+r_2\cos(q_1+q_2) & r_2\cos(q_1+q_2) & 0 \\ 0 & 0 & 1 \end{bmatrix} \tag{11}$$

Where, $\theta_1 = q_1$, $\theta_2 = q_2$, and $d_4 = q_3$.

Using this kinematics model, the PI controller computes the necessary torque applied to each DC servomotor in order to move the SCARA robot from the current position to the next target position. In order to obtain the inverse kinematics model in the SCARA robot, we must consider different methods, selecting the most adequate one in accordance with model considerations. In this work, we consider the analytical inverse kinematics model, to transform the output position into a joint coordinate. By solving Eqs. (12), (13) and (14) using Kramer's rule [13]:

$$\theta_1 = \tan^{-1}\frac{p_y\left(r_1+r_2\cos(\theta_2)\right)-p_x\left(r_2\sin(\theta_2)\right)}{p_x\left(r_1+r_2\cos(\theta_2)\right)+p_y\left(r_2\sin(\theta_2)\right)} \tag{12}$$

$$\theta_2 = \cos^{-1}\frac{\left({p_y}^2+{p_x}^2\right)-\left(r_1^2+{r_2}^2\right)}{2r_1r_2} \tag{13}$$

$$d_4 = d_1 - p_z \tag{14}$$

In order to compute the inverse kinematics model, we use the inverse Jacobian matrix:

$$\begin{bmatrix} \dot{q}_1 \\ \dot{q}_2 \\ \dot{q}_3 \end{bmatrix} = \left|J(q_i)\right|^{-1}\begin{bmatrix} \dot{p}_x \\ \dot{p}_y \\ \dot{p}_z \end{bmatrix} \tag{15}$$

Then, by using Eqs. (11), (12), (13), (14), and (15), we would obtain Eqs. (16) or (17), where $\dot{q}_2 = 0$ for $\Delta = 0$:

$$\begin{bmatrix} \dot{q}_1 \\ \dot{q}_3 \end{bmatrix} = \begin{vmatrix} \dfrac{1}{-\left(r_1\sin(q_1)+r_2\sin(q_2)\right)} \\ 1 \end{vmatrix}\begin{bmatrix} \dot{p}_x \\ \dot{p}_z \end{bmatrix} \tag{16}$$

Or,

$$\begin{bmatrix} \dot{q}_1 \\ \dot{q}_3 \end{bmatrix} = \begin{vmatrix} 1 \\ \overline{(r_1 \cos(q_1) + r_2 \cos(q_2))} \\ 1 \end{vmatrix} \begin{bmatrix} \dot{p}_x \\ \dot{p}_z \end{bmatrix} \tag{17}$$

From this subsection, it is obviously seen that the trajectory coordinate can be investigated for known angles of the joints (Kinematics model). Also, investigating can be done for joint angels (inverse Kinematics model). Thus, the position of each joint can be controlled individually, the SCARA robot can possess continuous motions in all directions. By using the inverse kinematics, the speed of each joint can be calculated, and its derivative with respect to time can be obtained.

2.2 SCARA robot control strategy

The general schematic of the control strategy used in this paper is shown in Fig. 3 in block diagram form. The actuators considered in this study are four identical DC servomotors (DC motor 1, 2, 3, 4) having the same parameter values coupled with a SCARA robot, which are composed by gears (gear 1, 2, 3…) for reducing spin speed and increasing torque in the drive shift. The input of each DC motor $v_{1,2,3...}$ is computed from each PI controller in the function of joint position errors ($\Delta q_{i,...}$). In our case of study, DC motors are used for both vertical (d_4) and horizontal ($\theta_{1,2,3}$) motions. Feedback position circuits are designed in order to compute the actual position of each controlled joint obtained from encoders with the desired positions calculated from the inverse kinematics model for known end effector's position $P(P_X, P_y, P_z)$.

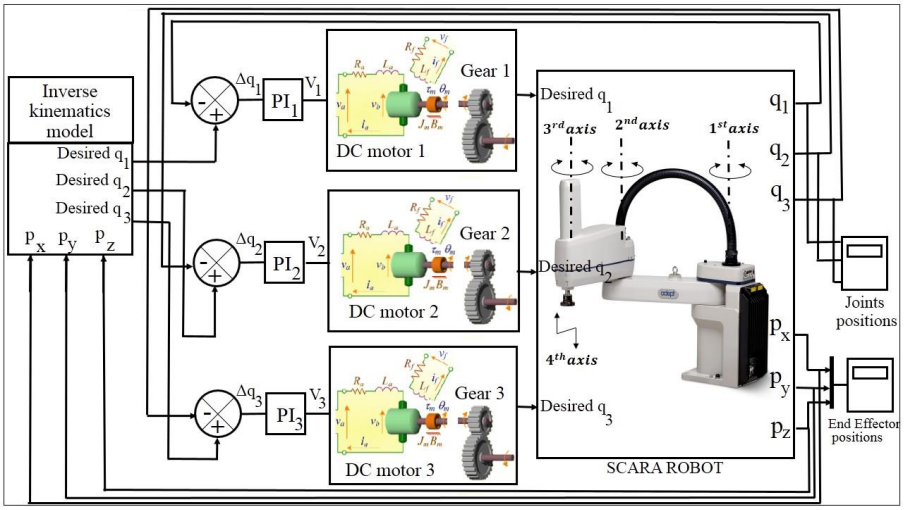

Fig. 3. SCARA robot modelling with feedback position control.

Such a control strategy leads to good trajectory tracking accuracy even in the presence of unknown disturbances. In this case of study, SCARA robot is constructed to achieve drilling operation of three mechanical objects in three different positions $P_i(P_{X_i}, P_{y_i}, P_{z_i})$. Nevertheless, faults can be caused by the robot manipulator itself and by particular environmental conditions. They can occur in a particular component of the system. The latter cause critical situations to the system operators and to the system itself. Consequently,

it is fundamental to include in the controller block (see Fig. 3) a block dedicated to detect and isolate the faults in the SCARA robot system. This block should have the capability to make a prompt diagnosis of the fault events. The next section describes the proposed fault diagnosis strategy.

3 Robust diagnosis to parameter and measurement uncertainties

Using the quantitative model-based method, the first step generates a set of residuals which is the results of ARRs. These fault indicators express the difference between the information provided by the actual system and that delivered by its reference operation model describing the normal operation [14]. The residuals characterize the system operating modes that are equal to zero in the fault-free case and different from zero in the faulty situation. Nevertheless, in presence of uncertainties that it can be due to a bad estimation of dynamics in a system, a variation of their values because of time or working conditions, or non-precise identification of the numerical values, these residuals are not exactly zero, this may cause false alarms on fault detection, so, these residuals should remain bounded between thresholds in normal operation, and these thresholds must be crossed in faulty situation. Noting that the difference between the parameter faults and the parameter uncertainties is that the parameter fault is considered as a parameter variation that exit the accepted range. In the other hand, the parameter uncertainty is considered as an accepted variation of the parameter in an accepted range. More details about the uncertainties modelling and generation using quantitative model-based method can be found in [15-17].

In the present work, we propose an algorithm of fault diagnosis of SCARA robot by considering the presence of both parameter and measurement uncertainties in order to improve the performance in terms of the robustness and fault diagnosis capabilities, and consequently, to ensure the safety able to detect and isolate faults. In general, an ARR is represented as a constraint that depends on the parameters of the system, the measurements, and the known inputs. These ARRs consist of two perfectly separate parts, a nominal part called residual (r) that describe the system operating, and an uncertain part, which is used for thresholds generation. The nominal part:

$$ARR_n = f(SSf, SSe, MSf, MSe, Sf, Se, u, \rho_n)$$

The uncertain part

$$a_n = f(\delta_\rho \rho_n, SSe, SSf)$$

Where ρ_n is the nominal part of the parameter, and δ_ρ is the parameter uncertainty, SSf and SSe are the flow and the effort inputs respectively. Sf and Se are the flow and the effort sensors respectively.

In determinist case, ARRs generation algorithm of robotic systems is based on the generation of the residuals. This approach is extended in this work to uncertain models, ARRs is deduced by expressing the power conservation as mathematical expression, as follows:

When the elements have the same flow:

$$ARR: \sum e_{i_n} - \sum w_i = 0 \tag{18}$$

When the elements have the same effort:

$$ARR: \sum f_{i_n} - \sum w_i = 0 \tag{19}$$

The calculated ARRs from this step consists of two separate parts in Eqs. (20) and (21) respectively, the nominal part called r_i and the uncertain part which includes both parameters and measurement uncertainties called a_i .

$$\begin{cases} r_i = \sum e_{i_n} \\ a_i = \sum |w_i| \end{cases} \tag{20}$$

$$\begin{cases} r_i = \sum f_{i_n} \\ a_i = \sum |w_i| \end{cases} \tag{21}$$

Since the parameter uncertainties values cannot be quantified perfectly, they are estimated using the available information, such as parameter maximum value or standard deviation, in order to obtain the inequality. The measurement errors are considered as bounded random variables.

$$-a_i \le r_i \le a_i \tag{22}$$

3.1 Residuals and thresholds generation for SACARA robot

In this subsection, we validate the proposed method of robust fault diagnosis in the presence of uncertainties on four degrees of freedom SCARA robot.

Table 2. Nominal and uncertainties values considered for the SCARA robot.

Parameter	Physical name	Nominal value	Multiplicative uncertainties	Uncertainties value
K	Torque constant	$0.043 N.m/A$	δ_K	$0.004 N.m/A$
R_a	Motor resistance	8.13Ω	δ_{R_a}	0.5Ω
L_a	Motor inductance	0.085H	δ_{L_a}	0.005H
J_m	Motor rotor inertia	$0.03 Kg.m^2/rad$	δ_{J_m}	$0.03 Kg.m^2/rad$
f_m	Motor friction coefficient	$0.4 N.m.s/rad$	δ_{f_m}	$0.04 N.m.s/rad$
N	Gear constant	30	–	–

Where 4 ARRs can be generated for the electrical parts, and 4 ARRs for the mechanical parts including the dynamics of the robot in each actuated joint. Table 2 provides the details of various system parameters and parameter uncertainties. m_i represents the robot arm masses where $i = 1,...,4$.

$$ARR_n : U_{PI_n} - \frac{L_a di_n}{dt} - R_a i_n - k\omega_n = 0, \tag{23}$$

Where, $n = 1,..,4$ and n is the number of the actuated joints.

$$ARR_5 : ki_4 - f_m\omega_4 - \left(J_m + \frac{1}{N^2}\underbrace{\left(m_4\left(\frac{{L_4}^2 + {l_4}^2}{12} \right) \right)}_{J_{Z_4}} \right) \frac{d\omega_4}{dt} = 0, \tag{24}$$

$$ARR_6 : ki_3 - f_m\omega_3 - \left(J_m + \frac{1}{N^2}\underbrace{\left(m_3\left(\frac{R^2}{4} \right) \right)}_{J_{Z_3}} \right) \frac{d\omega_3}{dt} = 0, \tag{25}$$

$$ARR_7 : ki_2 - f_m\omega_2 - \left(J_m + \frac{1}{N^2}\underbrace{\begin{pmatrix} m_2\left(\frac{{L_2}^2 + {l_2}^2}{12} \right) + \\ m_3\left(\frac{R^2}{4} \right) + \\ m_3{r_2}^2 + m_2\left(\frac{{r_2}^2}{4} \right) \end{pmatrix}}_{J_{Z_2}} \right) \frac{d\omega_2}{dt} = 0, \tag{26}$$

Where, (L_4, l_4), and (L_2, l_2) are the width and the length of the end effector and Arm2, respectively. R is the section radius of Arm3. ω_n and i_n are the angular velocity and the current of each DC Motor in each controlled joint.

$$ARR_8 : ki_1 - f_m\omega_1 - \left(J_m + \frac{1}{N^2}\underbrace{\begin{pmatrix} J_{G_1} + J_{G_2} + m_1\left(\frac{r_1^2}{4} \right) + \\ \left(m_2 + m_3 \right)\left(r_1^2 + \frac{r_1^2}{4} \right) + \\ \left(m_2 + m_3 \right) r_1 r_2 \cos\theta_2 \end{pmatrix}}_{J_{Z_1}} \right) \frac{d\omega_1}{dt} = 0, \tag{27}$$

Where $J_{Z_1}, J_{Z_2}, J_{Z_3}$, and J_{Z_4} are the inertia of Arm1, Arm2, Arm3, and the end effector, respectively.

In this application, we considered only one actuated joint system because all of them have the same structural model. Then, according to the ARRs generation presented previously in this section, we obtain the following ARRs:

$$ARR_2 : U_{PI_2} - \frac{L_a di_2}{dt} - R_a i_2 - k\omega_2 + a_2 = 0 \tag{28}$$

$$ARR_7 : ki_2 - f_m\omega_2 - \left(J_m + \frac{1}{N^2} \underbrace{\left(\begin{array}{l} m_2\left(\frac{{L_2}^2 + {l_2}^2}{12}\right) + \\ m_3\left(\frac{R^2}{4}\right) + \\ m_3{r_2}^2 + m_2\left(\frac{{r_2}^2}{4}\right) \end{array} \right)}_{J_{Z_2}} \right) \frac{d\omega_2}{dt} + a_7 = 0 \tag{29}$$

Where, a_1 and a_7 represent the uncertain part of ARR_2 and ARR_7, respectively:

$$a_2 = W_{R_a} + W_{R_a|i_2} + W_{L_a} + W_{L_a|i_2} + k\zeta_{\omega_2} + W_k, \tag{30}$$

$$a_7 = k\zeta_i + W_k + W_{J_m} + W_{J_m|\omega_m} + W_{f_m} + W_{f_m|\omega_m} \tag{31}$$

Where $W_{R_a}, W_{L_a}, W_k, W_{f_m}$ and W_{J_m} represent the fictitious inputs of parameter uncertainties. $W_{R_a|i_2}, W_{L_a|i_2}, W_{f_m|\omega_2}$ and $W_{J_m|\omega_2}$ represent the measurement uncertainties. ζ_{i_2} and ζ_{ω_2} are the errors in the current and motor velocity sensors respectively.

4 Simulation results

After representing the SCARA manipulator model including the DC motor actuator dynamics in each joint, establishing the controller to be used, and the proposed algorithm of fault diagnosis in presence of both parameter and measurement uncertainties, a test trajectory was determined in the space to subject SCARA robot to path tracking (drilling operation of three mechanical objects in three different positions). This trajectory is shown in Fig. 4. The end effector trajectory according to time is shown in Fig. 5. Fig. 6 shows the angular position of each controlled joint.

The residuals r_1 and r_2 which is the numerical evaluation of ARR_2 and ARR_7 are bounded by ($|a_2|$ and $|a_7|$) and ($-|a_2|$ and $-|a_7|$) respectively. These residuals with adaptive thresholds are represented as expected in Fig. 7. The two residuals are close to zero and do not exceed the adaptive thresholds. This means that the system is healthy. However, since we do not the same measurement system the obtained thresholds are not the same, which implies different sensitivities, and consequently different thresholds.

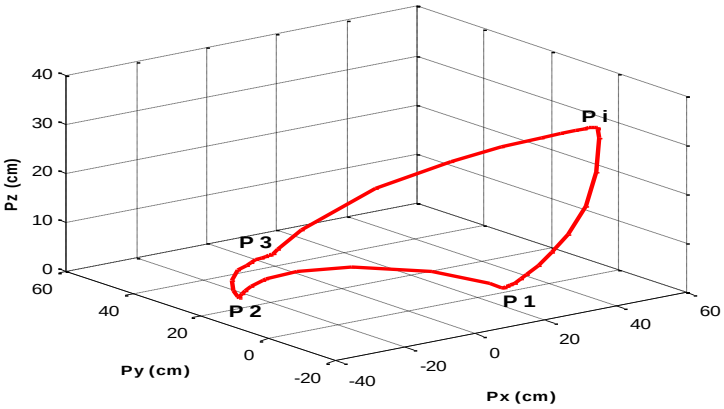

Fig. 4. SCARA robot end effector Cartesian trajectory when subjected to healthy conditions.

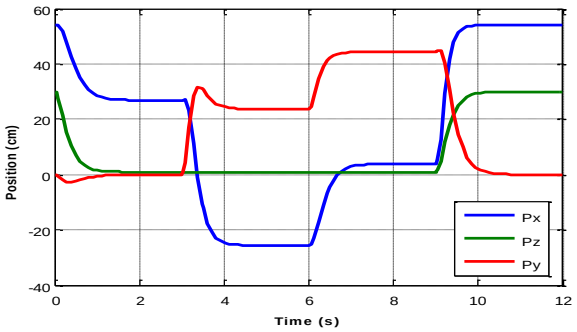

Fig. 5. End effector trajectory positions according to time.

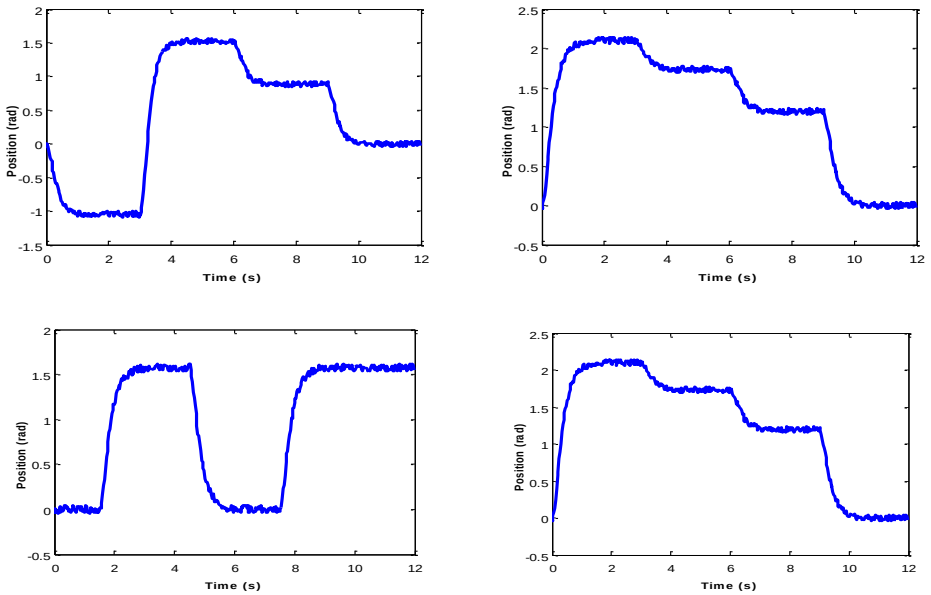

Fig. 6. Angular positions of the controlled joints.

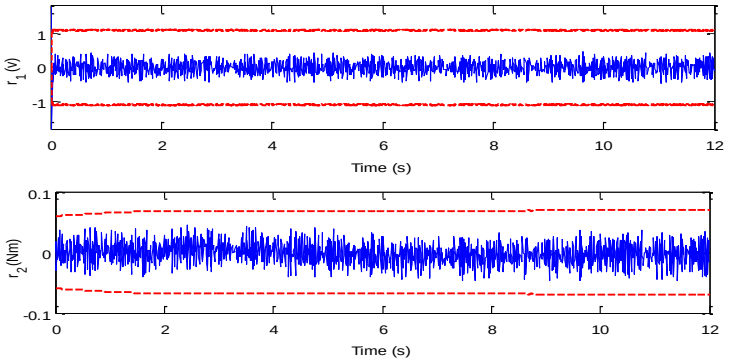

Fig. 7. r_1 and r_2 in nominal conditions .

An additive fault is then introduced in the current sensor equivalent to 0.6A at time t=6s. In this case, the response of the residuals r_1 and r_2 are given in Fig. 8. We remark that this fault is clearly detected by these residuals because they exceed the adaptive thresholds. Moreover, this fault is estimated using the algorithm developed in [18], by two ways in Fig. 9.

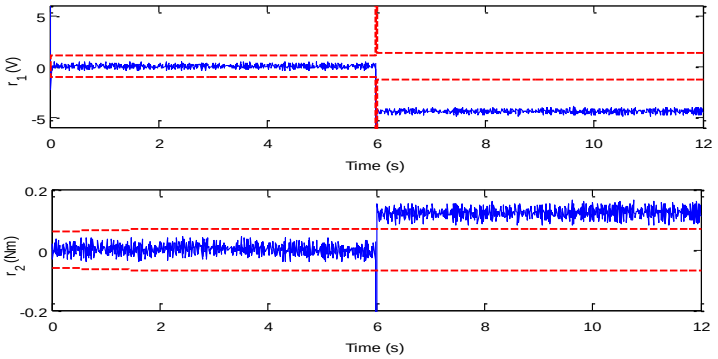

Fig. 8. r_1 and r_2 in case of current sesnor fault.

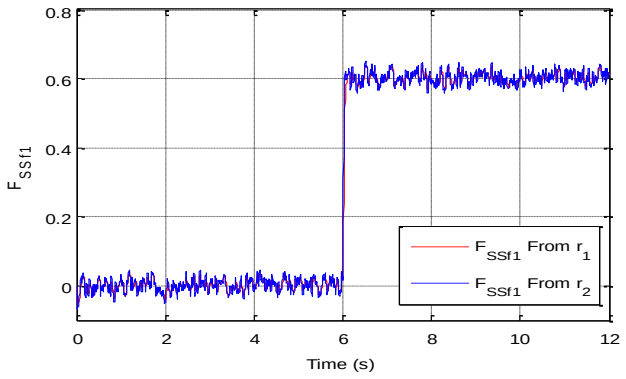

Fig. 9. Estimated current sensor fault magnitude.

Another scenario consists of testing the developed method in the presence of a parameter fault. Hence, a fault in the electrical resistance parameter (2Ω), is also introduced at 6s. From Fig. 10, it can be seen that the SCARA robot end-effector trajectory with an electrical resistance fault (blue dashed line) deviates from that in the fault-free case (red solid line), and does not complete either a trajectory in the suited time or all drilling operations, because the power generated by this fault change the dynamics of the physical system. Nevertheless, in the presence of current sensor fault, the trajectory does not deviate from the desired trajectory, because a fault in a diagnosis sensor does not change the power in the physical system, it modifies only the information used to calculate the residuals. The electrical resistance parameter fault is detected by the residual r_1, while the residual r_2 does not detect this fault because it is not sensible to it (Fig. 11). The estimation of this fault is given by Fig. 12.

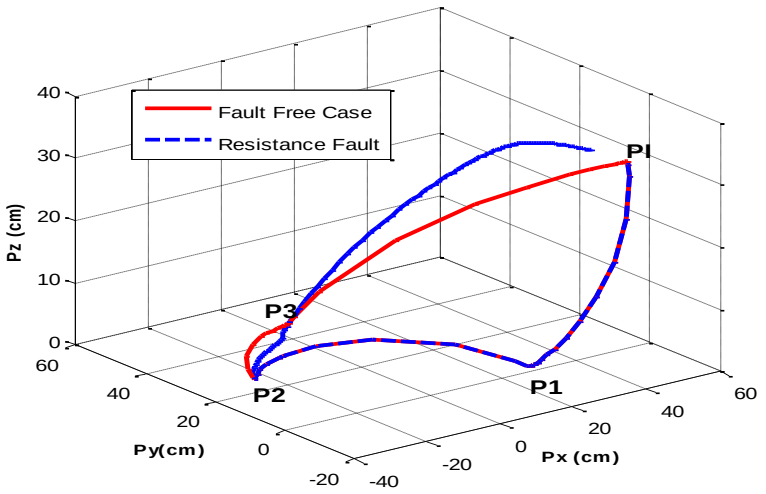

Fig.10. SCARA robot end effector Cartesian trajectory when operating under normal and faulty conditions .

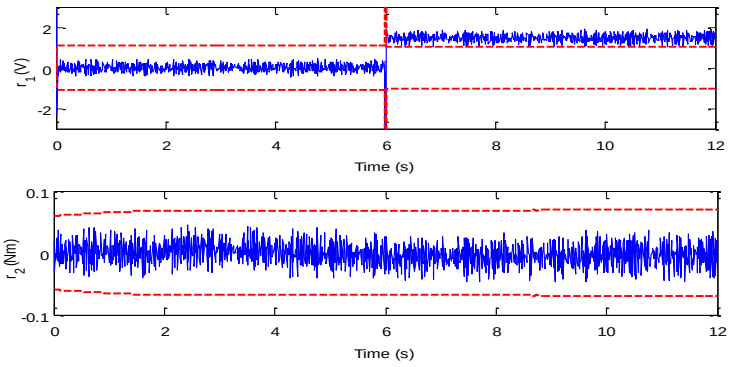

Fig.11. r_1 and r_2 in case of R_a parameter fault.

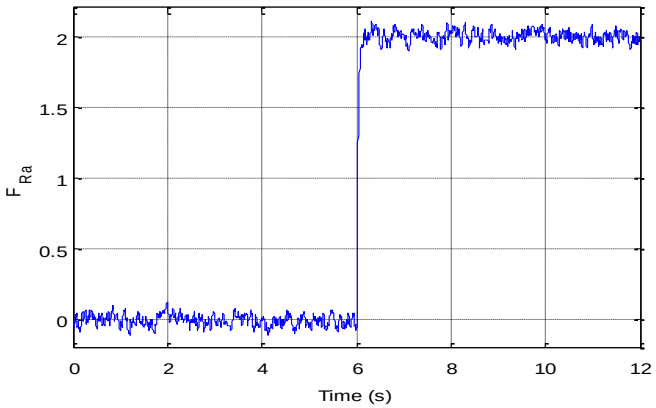

Fig. 12. Estimated parameter fault magnitude.

5 Conclusion and future works

The goal of this paper was to present a robust fault diagnosis approach on a SCARA robot in the presence of both parameter and measurement uncertainties. This approach is based on the use of the quantitative model-based method to generate residuals and adaptive thresholds. The proposed robot is created using SolidWorks program and Matlab/Simulink software to obtain the system dynamic behaviour. Analytical forward and inverse kinematics solutions were derived by using the Denavit-Hartenberg approach. DC servomotors driving each of the robot arm joints is modelled and considered in the closed-loop control. Then, the PI controllers have been used to control the angular position of these robot joints, so that flow the desired trajectory. Simulation results were presented for a SCARA robot and demonstrated the ability of the proposed method to detect the faults in the presence of uncertainties and determine the nature, and the magnitude of the fault.

The physical phenomena like a motor friction coefficient that deviate from the natural variations based upon different operational conditions, its unidirectional variations are not taken into consideration, this must be solved in the future work by using the so-called interval-valued uncertainties generation.

References

1. Z. Gao, C. Cecati, S. X. Ding, IEEE Trans. Indus. Electro **62**, 3757 (2015).
2. K. Tidriri, N. Chatti, S. Verron, T. Tiplica, Ann. Reviews. Contr **42**, 63 (2016).
3. A. A. Jaber, R. Bicker, American. J. Mech. Enginee **4**, 21 (2016).
4. F. Piltan, M. Sohaib, JM. Kim, *In: Kim JH. et al. (eds) Robot Intelligence Technology and Applications 5. RiTA 2017. Advances in Intelligent Systems and Computing, Springer, Cham,* **751** (2017).
5. M. S. Khireddine, K. Chafaa. N. Slimane, A. Boutarfa, Fault diagnosis in robotic manipulators using Artificial Neural Networks and Fuzzy logic *In: 2014 World Congress on Computer Applications and Information Systems (WCCAIS), IEEE* 1-6 (January 2014).
6. L. M. Capisani, A. Ferrara, A. Ferreira de Loza, L. M. Fridman, IEEE Trans. Indus. Electro **59**, 3979 (2012).

7. Y. Zeng, Y. R. Xing, H. J. Ma, G. H. Yang, *In The 27th Chinese Control and Decision Conference (2015 CCDC) IEEE*, 6569-6574 (May 2015).
8. H. J. Ma, G. H. Yang, Infor. Scien **366**, 12 (2016).
9. J. Chen, R. J. Patton, *Springer Science and Business Media* **3**, (2012).
10. M. T. Das, L. C. Dülger, Simu. Model. Practi. Theory **13**, 257 (2005).
11. C. Urrea, J. Kern, Inter. J. Adva. Robo. Syst **9**, 58 (2012).
12. S. M. Said, A. S. Ismail, I. Baharin, *In 2014 11th International Conference on Ubiquitous Robots and Ambient Intelligence (URAI) IEEE*. 397-402, (November 2014).
13. M. S. Alshamasin, F. Ionescu. R. T. Al-Kasasbeh, Euro. J. Scien. Resear **37**, 388 (2009).
14. A. K. Samantaray, B. O. Bouamama, *Springer Science and Business Media*, (2008).
15. Y. Touati, R. Merzouki, B. O. Bouamama, Mechat **22**, 1148 (2012).
16. Y. Touati, M. A. Mellal, D. Benazzouz, ISA trans **62**, 299 (2016).
17. M. S. Jha, G. Dauphin-Tanguy, B. Ould-Bouamama, Cont. Enginee. Prac **71**, 61 (2018).
18. Y. Touati, B. O. Bouamam, R. Merzouki, *In 2012 7th IEEE Conference on Industrial Electronics and Applications (ICIEA) IEEE*, 1236-1241 (July 2012).